Efficient Preconditioned Soil–Foundation–Structure Interaction Approach to Compute Tall-Building Time Periods

A. M. Elmeliegy[1] and Youssef F. Rashed[2]

Abstract: The present paper suggests an efficient preconditioned two-iteration substructure approach—namely, preconditioned soil–structure interaction (PSSI)—to couple the analysis of a superstructure over fixed bases (which is traditionally carried out in design companies) with the analysis of foundation plates over an elastic half-space (EHS) to obtain more accurate equivalent supporting spring stiffnesses. Hence, an accurate building time period and, consequently, lateral loads could be computed. The effectiveness of the proposed approach is illustrated in several numerical examples in terms of number of iterations and scalability followed by comparison with previous work to demonstrate the superiority of the proposed approach. **DOI: 10.1061/(ASCE)SC.1943-5576.0000422.**

Author keywords: Soil–structure interaction; Iterative coupling; Tall buildings; Time period; Lateral loads; Base shear.

Introduction

In the analysis of tall buildings, it is common—in practice—to model the superstructure separate from the raft–soil substructure. In this case, the analysis is usually carried out using the fixed-base model, which implicitly assumes that the foundation soil is infinitely rigid. This is basically due to the limitation of storage and the need for affordable computational time. Such simplifications are not good enough to capture the true behavior of buildings on raft foundations, especially due to dynamic loading. Gazetas and Mylonakis (1998), Mylonakis and Gazetas (2000), and Bhattacharya et al. (2004) have confirmed that the soil–structure interaction plays an important role in the behavior of the buildings. Also, Jayalekshmi and Chinmayi (2014, 2016) demonstrated the significant effect of considering the foundation–soil flexibility on the dynamic characteristics, such as building time periods and natural frequencies. Consequently, seismic demands will be affected (i.e., the base shear and lateral deflection). The same conclusions were confirmed by Viladkar et al. (2006) and Mengke et al. (2014).

Historically, there are many approaches to modeling the soil–structure interaction problem, and we cannot point to all of them here for the sake of clarity. However, we present the most known methods that are often used in practice and are well known to most of engineers:

1. Winkler's model (Winkler 1867), the multiparametric model (Kerr 1964), and the modified Winkler model by Gazetas (1991) are among the available simplified approaches in which the soil is treated as springs. In such approaches, the stiffness values of springs are determined based on empirical equations (Horvath 1983; Bowles 1986; Colasanti and Horvath 2010). Despite the simplicity of these approaches, they possess a major deficiency in that the spring stiffness is not a physical property of the soil, such as Young's modulus (E). Moreover, and most importantly, these approaches do not consider the equivalent spring stiffness to be frequency dependent in the case of dynamic analysis (Gazetas 1991; Mylonakis et al. 2006; Kalkan and Chopra 2010).
2. After the advancements in the FEM, and with the fast progress in computer technology, the full three-dimensional continuum (3D FEM model) approach came into the picture as a refined soil representation. In this approach, the superstructure, foundation, and soil are modeled all together monolithically and are analyzed simultaneously (Fig. 1). Whereas the superstructure and the foundation are modeled using the conventional one-dimensional (1D) and two-dimensional (2D) elements (such as beam and shell elements), the soil continuum is modeled using the 3D solid elements. One of the advantages of this approach is that it can be used for complex geometries and different material properties. Also, it can be used for nonlinear interaction analysis. However, the main advantage of this model is that it takes into consideration the interaction between the soil substructure and the structure itself directly in one step without any iterations (direct method), which simulates the reality. Moreover, the soil parameters, such as Young's modulus (E) and Poisson's ratio (ν), are considered, which are among the soil physical properties. However, for large-scale buildings, in addition to the huge modeling effort, the number of degrees of freedom (DOFs) can easily reach the multimillions, and such problems need a very high computational time and large storage space. Therefore, this method is rarely used in practice.
3. A better and simpler representation of 3D semi-infinite soil is represented by Mindlin's (Wang et al. 2001) in the form of elastic half-space (EHS). This model can replace modeling of the soil as 3D by an equivalent 2D interface (Shaaban and Rashed 2013). Unlike Winkler's model and the two-parameter model, the EHS model uses data obtained from geotechnical investigations (E, ν). Unfortunately, apart from Shaaban and Rashed (2013), such a model is not implemented in any commercial software to analyze the raft over EHS.

The poor accuracy of the Winkler model representation and the high modeling and computational limitations of the full 3D

[1]Ph.D. Student, Dept. of Civil, Construction, and Environmental Engineering, North Carolina State Univ., 407 Mann Hall, 2501 Stinson Dr., Campus Box 7908, Raleigh, NC 27695 (corresponding author). Email: aaelmeli@ncsu.edu

[2]Professor, Structural Engineering Dept., Faculty of Engineering, Cairo Univ., Cairo 12613, Egypt. Email: youssef@eng.cu.edu.egin

Note. This manuscript was submitted on September 8, 2018; approved on December 14, 2018; published online on April 3, 2019. Discussion period open until September 3, 2019; separate discussions must be submitted for individual papers. This paper is part of the ***Practice Periodical on Structural Design and Construction***, © ASCE, ISSN 1084-0680.

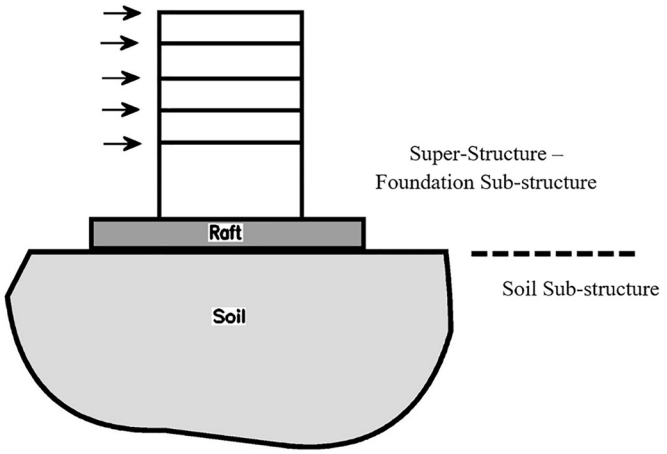

Fig. 1. Full 3D continuum model.

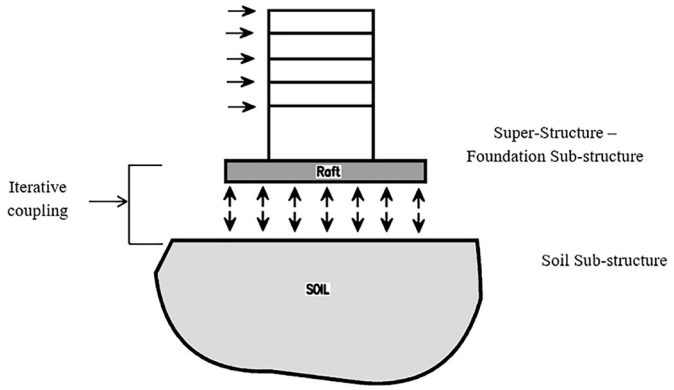

Fig. 2. Conventional iterative substructuring approach.

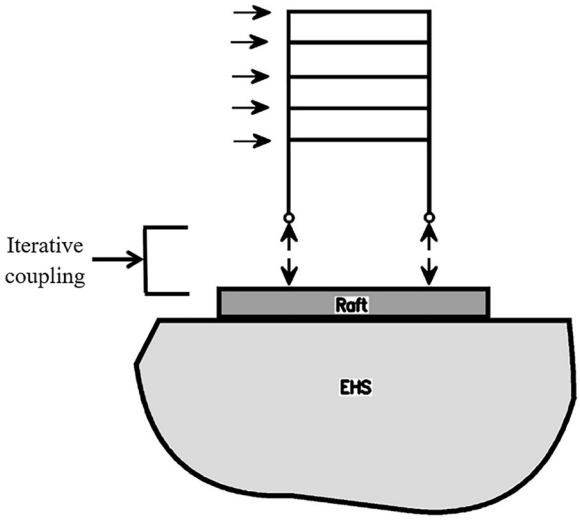

Fig. 3. Proposed substructuring approach.

continuum model were the motivation for developing a more accurate and efficient model that could be used in practice: the substructuring approach. In the substructuring approach, the soil–foundation–structure interaction problem is split into two independent parts; the superstructure part includes the foundation and the soil part (either as a 3D model using solid elements or as the EHS model). The coupling between the superstructure and the soil part is carried out using different methods that require excellent knowledge of matrix analysis of structure and static condensation. Basically, these methods evaluate (condense) the super- and subdomain stiffness matrices at the interface with the soil. By solving the interface problem and then solving the super- and subdomains problems, the effect of the soil–structure interaction can be taken into consideration (Huang et al. 2015; Kocak and Mengi 2000). However, evaluating the interface stiffness matrix—which is naturally dense because it includes the inversion of the stiffness matrix of the condensed part—in terms of the other DOFs (superstructure and soil DOFs) is not a trivial task and requires high computational time and storage because there are too many condensed DOFs, especially in large-scale buildings (usually multimillions). Although this approach, unlike the full 3D continuum approach, requires less modeling effort and computational time, it still needs relatively high computational time and storage that can handle the condensation process. Hence, this method is not presented in any practical software that can be used by engineers; therefore, it is also not suitable in practice.

To overcome the shortcomings of the previous method caused by the inversion process of the static condensation of a large number of DOFs, a substructuring approach based on iterative technique was developed. To the best of our knowledge, the iterative substructuring approach was presented for the first time by Hemsley (1987) in which the soil was treated as an EHS. This approach is similar to the aforementioned substructuring approach; however, the coupling between the superstructure (building and raft) and the substructure (soil as EHS) is carried out in an iterative manner. Recently, this approach was modified as demonstrated by Pandey et al. (1994) and Jahromi et al. (2009) in which soil was treated as a 3D continuum (Fig. 2). In this approach, the building, including the raft foundation, is assumed to be resting on Winkler's springs. The Winkler spring stiffness is initially calculated using empirical equations as by Pandey et al. (1994). The whole building is analyzed, and the spring forces are determined. Spring forces are then applied to the soil continuum model. The soil model is then analyzed, and the deformations are determined at the load locations. Using the load-displacement relationship, new stiffness values for springs can be calculated. This process is repeated using different techniques till the convergence is achieved (Pandey et al. 1994; Jahromi et al. 2009). Similar convergence being considered in the practice of design companies by limiting the relative error in the spring forces between two successive iterations to be within 5–7% (Dang et al. 2013). In general, and based on numerical examples presented here, this approach requires approximately 10–12 iterations to converge to an acceptable tolerance.

The main disadvantage of this approach is that the interface problem results from placing the separation cut between the superstructure and the soil subdomain [i.e., the raft–soil interface is typically dense (large number of DOFs; hence, large number of Winkler's springs)]. Hence, producing a large linear system that makes the iterative process converge slowly, especially for large-scale problems where a large number of unknowns come into the picture, depends on the problem and mesh size. This means that this methodology can be used for a small problem effectively but is still not scalable (difficult to converge for larger problems).

The outline of the remainder of the paper is as follows. First, we present the idea of the proposed technique, followed by a section on remarks and limitations. Then, we present the procedure of that

technique as detailed steps. The next section contains an array of numerical examples that demonstrate the performance of the proposed technique and its accuracy and efficiency compared to the old techniques. Then, we demonstrate the implementability in practice and how engineers can make use of the presented technique. Finally, we present a discussion and concluding remarks about the main strong points of the presented technique with some recommendations for further research in this area.

Proposed Substructuring Approach: Preconditioned Soil–Structure Interaction

In this paper, a new approach based on iterative substructuring is presented. The proposed approach suggests splitting the entire structure into two separate parts: the superstructure and the raft–soil substructure. Notice that in this approach, the separation cut is placed in a different way than in the conventional iterative substruc-

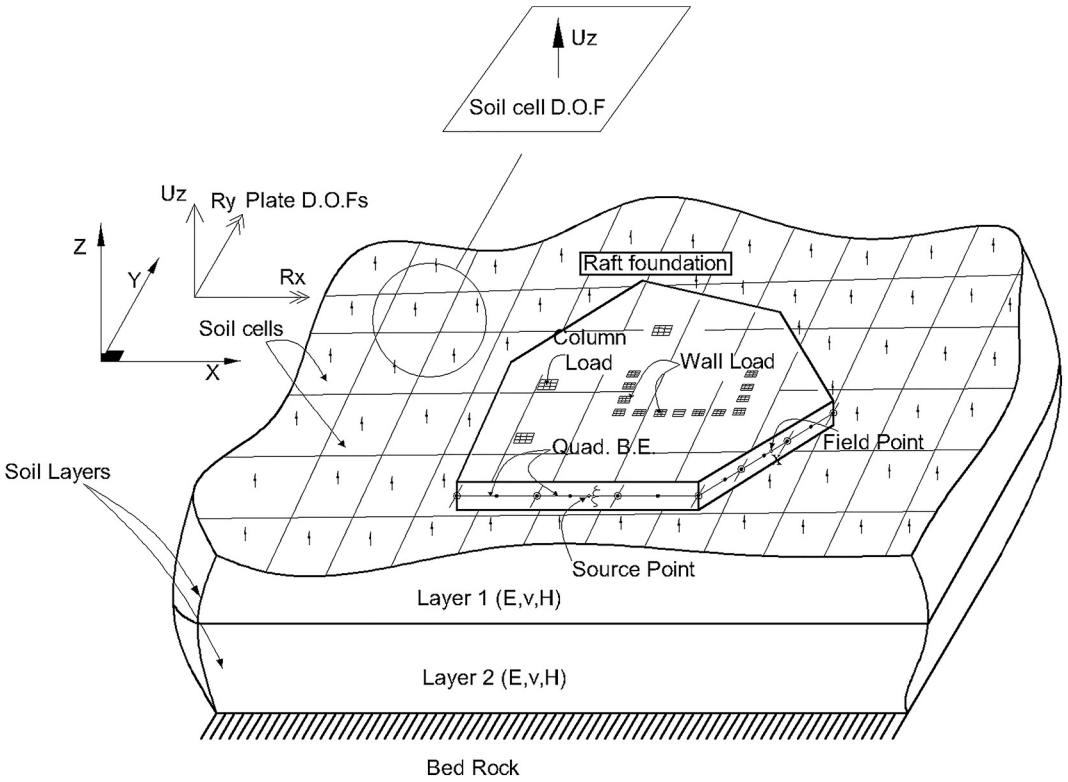

Fig. 4. PLPAK-EHS problem representation. B.E. = Boundary Element.

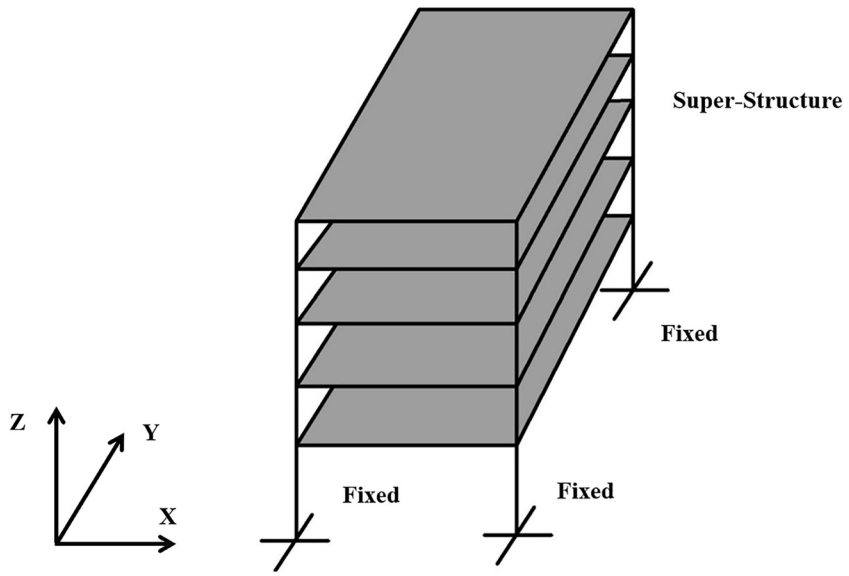

Fig. 5. Building model on fixed base.

Pract. Period. Struct. Des. Constr., 2019, 24(3): 04019007

turing approach. In other words, the separation cut between the two substructures is proposed to be placed at the column face at the top foundation level (Fig. 3). This is considered as a preconditioner for the soil–structure interaction problem, hence the name preconditioned soil–structure interaction (PSSI) technique. This reduces the number of DOFs dramatically, limiting them to the number of vertical supporting elements (columns and shear walls) compared to the conventional iterative substructuring technique described previously in the "Introduction." This leads to a reduction in the size of the interface problem, and hence, faster convergence. In addition, the simple procedure steps and the ease of implementation make this approach much more superior to the other methods in the literature.

The proposed approach also makes use of the available software that is commercially used to model superstructures, such as the ETABS software (Computers and Structures Inc. 2011). In contrast, the foundation–soil coupled system is proposed to be analyzed using the PLPAK software (Rashed 2005).

The PLPAK software is for structural analysis of building slabs and foundations. It is based on the direct boundary element method of the shear-deformable plate theory according to Reissner (Reissner 1947; Vander Weeën 1982). which is suitable

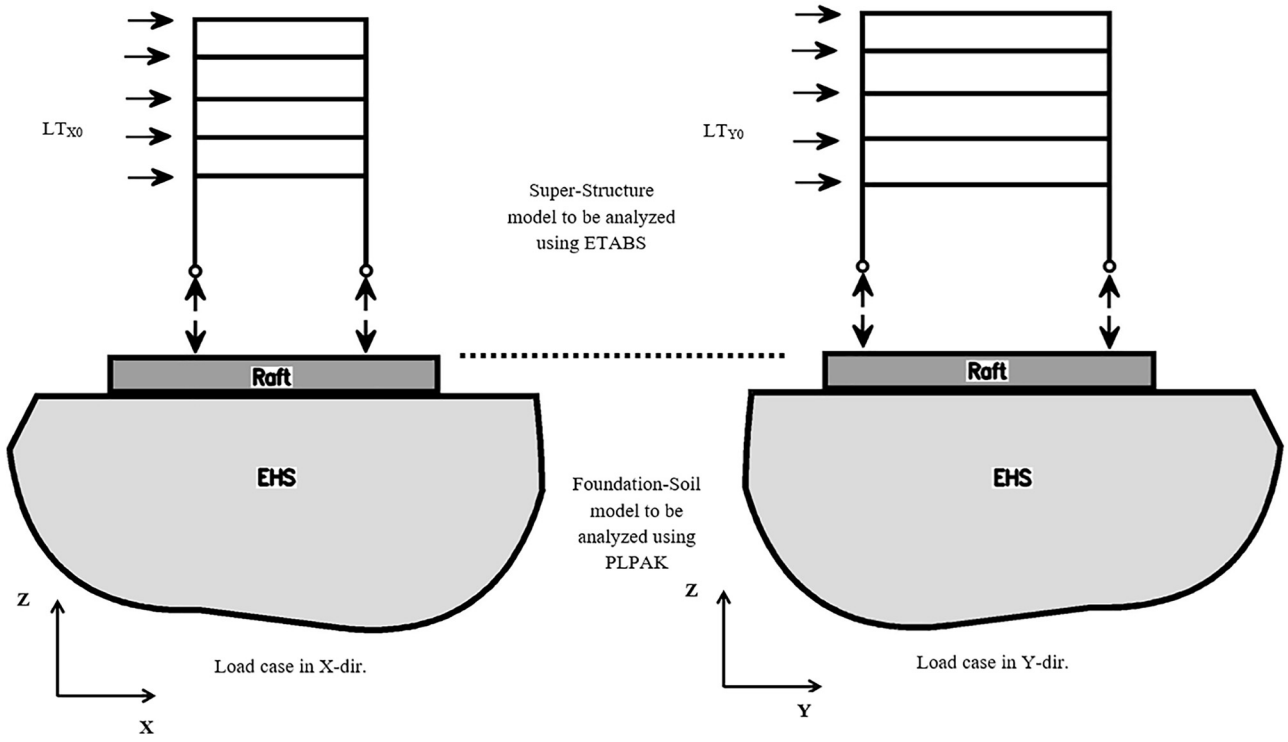

Fig. 6. Step 1 in proposed coupling iteration in *X*- and *Y*-directions.

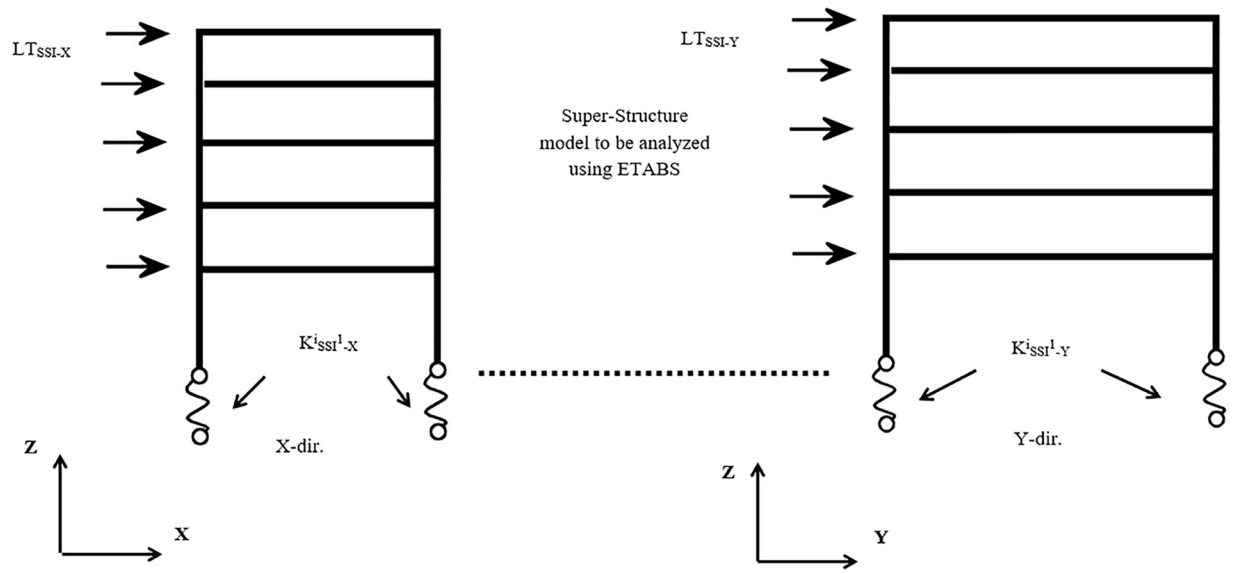

Fig. 7. Modified superstructure model after Iteration step 1 in *X*- and *Y*-directions. LT = lateral loads.

Pract. Period. Struct. Des. Constr., 2019, 24(3): 04019007

for structural foundations. Recently, PLPAK became able to solve foundations over EHS (Shaaban and Rashed 2013). It has to be noted that this technique is applicable to any EHS software without losing generality.

Limitations and Remarks

This technique depends on the availability of any two software programs (one for the superstructure and the other for analysis of the foundation–soil system). Therefore, the main limitation is the availability of such software to the practitioners. Once those software programs are available, this technique can be implemented easily. This technique is proposed Elmeliegy and Rashed (2017) in a form of software available at BE4E (2017) with simple but efficient graphical user interface (GUI). ETABS 9.7.4 was used in this study. Slight changes in the source codes would be implemented to be compatible with the newer versions if requested. However, the method is general and can be implemented for any two similar software programs. Also, soil damping and nonlinearity are not presented in this work and are the subject of further research. Some other important remarks follow.

Remark 1: Effect of Rotational and Horizontal DOFs

It has to be noted that we considered only the vertical DOFs in the coupling process (enforcing the continuity for vertical DOFs only). We tested several numerical examples and found that the dominant DOFs in the coupling were the vertical DOFs, and the other DOFs (rotational and horizontal DOFs) together contributed less than 5% of the case considering all DOFs together in the coupling. The rotational and horizontal DOFs can be taken into consideration but need some complicated analyses because they may cause numerical instabilities in the model, and that can be studied in other research. However, we only present the numerical example, only taking the vertical DOFs into consideration for the sake of clarity.

Remark 2: Column Load Representation

We have to mention that the application of the column loads on the raft foundation does not act at a single point. Instead, the column load is divided by the area of that specific column and is applied as a stress (force/unit area), as presented in Fig. 4. Although this was not the main aim of the study, it is definitely more accurate than presenting the loads on the raft as a concentrated load. Again, this method

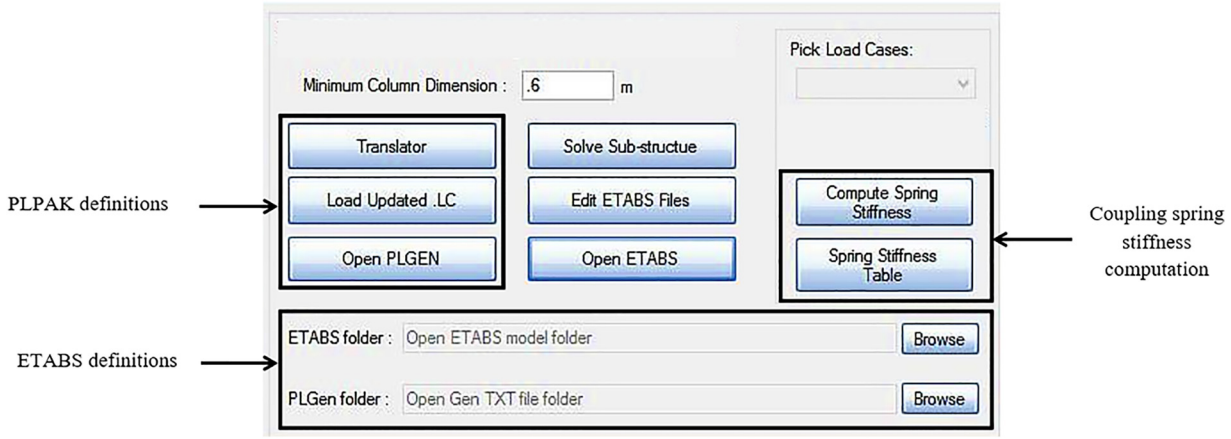

Fig. 8. GUI of the proposed approach.

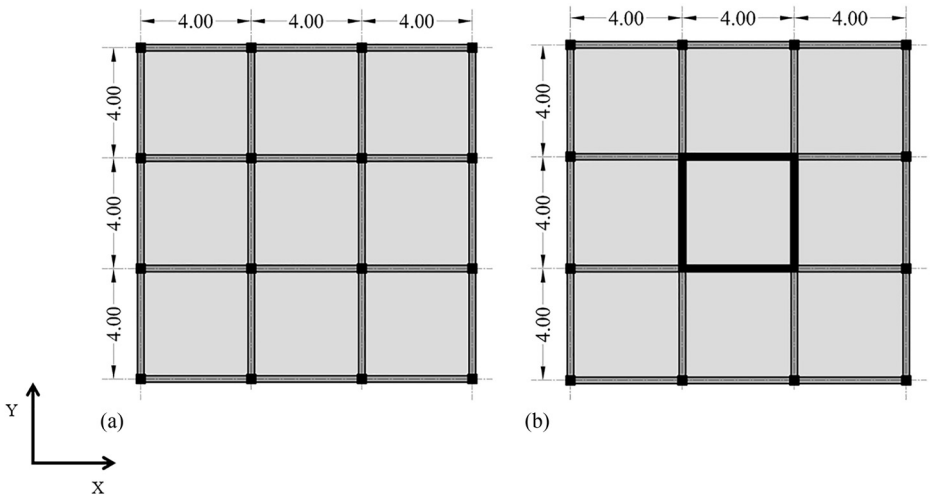

Fig. 9. Structural layout and dimensions: (a) bare frame; and (b) frame with shear wall.

Pract. Period. Struct. Des. Constr., 2019, 24(3): 04019007

can be applied to any two software programs that have similar capabilities without losing generality.

Remark 3: Wall Load Representation

As an approximation of the wall load, we considered that the wall consisted of a number of adjacent columns, hence the wall load can be easily represented as the number of adjacent column loads as in Remark 2, as seen in Fig. 4.

Although the examples used in this study were either fully symmetric about the two major axes in the plane or partially symmetric about only one major axis, or even to some extent fully nonsymmetric, such as in the last example in the "Numerical Examples" section, for all cases the number of iterations to achieve a satisfactory convergence was two. However, this may not be the case of more complex planes, where the system becomes more nonsymmetric and the rotational DOFs come into the picture (especially the torsional DOFs). However, as demonstrated in Remark 1, we can always take only the vertical DOFs into consideration while the other DOFs are restrained, and that effectively captures most of the soil–foundation flexibility; this way, the whole system is decomposed into a similar system discussed in this paper. This always ensures that the number of iterations is minimal because the iteration is carried out only on the vertical DOFs.

Table 1. Cross-sectional dimensions

Number of stories	Column dimensions (m)		Shear-wall thickness (m)
	Up to third story	Above third story	
4	0.32×0.32	0.32×0.32	0.15
16	0.6×0.6	0.5×0.5	0.25

Table 2. Soil properties

Description	Poisson's ratio	Young's modulus [E (kN/m^2)]
Rock	0.3	8.4×10^6
Dense soil	0.3	1.91×10^6
Stiff soil	0.35	4.46×10^5
Soft soil	0.4	1.03×10^5

Proposed Procedure for Evaluating Time Periods of Tall Buildings

In this section, we present the proposed procedure steps to compute tall-building time periods considering the effect of foundation–soil flexibility. Hence, more accurate and economic values of base shear and lateral loads could be computed. These procedures are presented as follows.

Step 0

1. The tall building is modeled and analyzed over the traditional fixed-column bases at the foundation top face (Fig. 5). Defining the masses participating in the lateral analysis, the analysis is carried out under the gravity loads [dead loads (DL) + part of live loads (LL)] to determine the mode shapes and the time periods in both directions [$T_{X(\text{fixed base})}$ and $T_{Y(\text{fixed base})}$].
2. Approximate values of lateral loads [LT_{X0} and LT_{Y0}] are then computed—based on the provision code that is relevant to the area of the building—in both directions (X and Y) based on the computed values [$T_{X(\text{fixed base})}$ and $T_{Y(\text{fixed base})}$], and hence, such values are applied to the superstructure model in separate load cases.

Step 1

1. For load cases in the X- and Y-directions, the column vertical reactions [$(F_i)_x$ and $(F_i)_y$, where i is the column number] are computed in the previous step. Hence, such loads are reversed and applied to the foundation plate–soil model.
2. The analysis is carried out for each direction (X and Y) for the foundation plate–soil model. The PLPAK software is used to compute vertical displacement in both load cases (X and Y) [i.e., $(\Delta_i)_x$ and $(\Delta_i)_y$] under the applied loads from the superstructure. It has to be noted that the soil is treated as a half-space 3D continuum.
3. The column fixed-end conditions are replaced by springs. This is carried out in each direction (X and Y). Each spring's stiffness in both directions ($K^i_{\text{SSI}^j\text{-}X}$ and $K^i_{\text{SSI}^j\text{-}Y}$, where j is the iteration number) is determined by dividing the column vertical reaction (obtained in Point 1) by the obtained vertical displacements (obtained in Point 2)

Table 3. Fundamental time periods (s)

Structural system	Soil type	4-story		16-story	
		3D FEM model (Jayalekshmi and Chinmayi 2014)	Proposed approach	3D FEM model (Jayalekshmi and Chinmayi 2014)	Proposed approach
Bare frame	Fixed	0.850		3.000	
	Rock	1.000	(+1.1%) 0.860 [–14%]	3.510	(+1%) 3.020 [–14%]
	Dense soil	1.000	(+2.1%) 0.868 [–13%]	3.520	(+6%) 3.170 [–10%]
	Stiff soil	1.000	(+2.4%) 0.871 [–13%]	3.550	(+8%) 3.240 [–9%]
	Soft soil	1.010	(+3.5%) 0.880 [–12%]	3.660	(+11%) 3.330 [–9%]
Frame with shear walls	Fixed	0.180		1.280	
	Rock	0.190	(+11%) 0.199 [+5%]	1.340	(+15%) 1.470 [+10%]
	Dense soil	0.220	(+39%) 0.250 [+13%]	1.460	(+26%) 1.610 [+10%]
	Stiff soil	0.290	(+72%) 0.310 [+7%]	1.760	(+51%) 1.930 [+10%]
	Soft soil	0.410	(144%) 0.440 [+7%]	2.250	(+78%) 2.280 [+1%]

Note: Values in parentheses indicate percentage with respect to the fixed-base model; values in brackets indicate percentage with respect to the 3D model by Jayalekshmi and Chinmayi (2014).

$$K^{i}_{SSI^1\text{-}X} = \frac{(F_i)_x}{(\Delta_i)_x} \quad (1a)$$

$$K^{i}_{SSI^1\text{-}Y} = \frac{(F_i)_y}{(\Delta_i)_y} \quad (1b)$$

4. These new springs are updated in the ETABS model of the superstructure. It has to be noted that there are two sets of vertical springs to represent two cases of loading: one in the X-direction and another in the Y-direction (Figs. 6 and 7).
5. The superstructure is then reanalyzed twice (in X-direction and in Y-direction) over the springs obtained in the former step with a mass participating ratio similar to those presented in Step 0.
6. The new mode shapes are obtained for each direction, and consequently, new improved time periods are determined ($T_{SSI^1\text{-}X}$ and $T_{SSI^1\text{-}Y}$) as in Fig. 7.
7. New improved values of lateral loads in each direction ($LT_{SSI\text{-}X}$ and $LT_{SSI\text{-}Y}$) are then computed and applied to the superstructure model. This completes the first iteration.

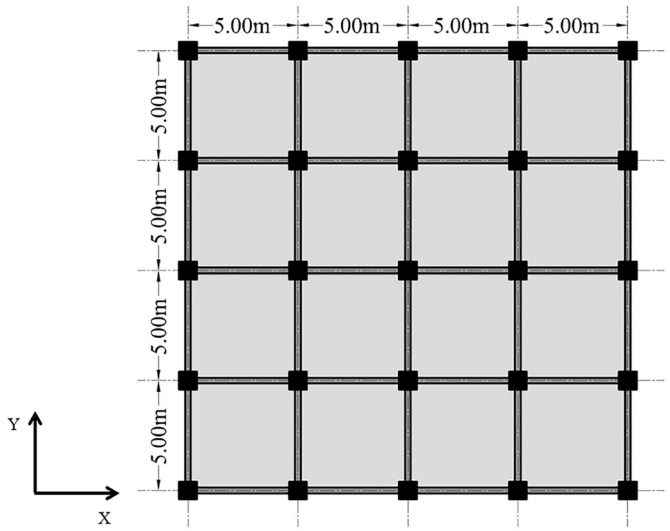

Fig. 10. Structural layout and dimensions.

Table 4. Section properties

Model	Beam size (cm)	Slab thickness (cm)	Column dimensions (cm)	Raft thickness (cm)
6-story	25 × 60	15	60 × 60	60
12-story	25 × 60	15	80 × 80	100

Table 5. Soil properties

Soil condition	Poisson's ratio	Modulus of elasticity [E (kN/m^2)]	K_z (Abdel Raheem et al. 2015) (kN/m^2/m)
Stiff soil	0.33	244,800	14,172.9
Medium soil	0.33	122,400	7,086.4
Soft soil	0.33	61,200	3,543.2

Step 2

Step 1 is repeated. The iterations are designed to be stopped when the values of the spring stiffness in each direction converge. Usually only two iterations are required, as we show in an array of numerical examples.

For the sake of practicality and to make it easy for usage by engineers in the analysis of buildings over raft foundations, we made a simple but efficient GUI named after the proposed approach (PSSI). Fig. 8 demonstrates the developed GUI, referring to the functionality of each button. The GUI in Fig. 8 was designed to carry out single coupling iteration (Step 0 to Step 2). However, it can be used by modelers in a recursive manner to carry out as many iterations as required because the convergence criteria and the acceptable tolerance will be decided by the users according to the problem and the code of provision.

Numerical Examples

In this section, several numerical examples are presented to demonstrate the effectiveness and accuracy of the proposed approach. The fundamental time periods obtained from the analysis using the proposed approach were compared to those of previously published results obtained using the 3D FEM and conventional substructuring iterative approaches available in practice. For all examples, the percentage of mass participation in the computation of time periods was considered to be the dead load plus 25% of the live load. Also, the material properties used for the superstructure were concrete with modulus of elasticity of $E = 2.21 \times 10^7$ kN/m^2, Poisson's ratio of $\nu = 0.2$, and weight per unit volume of $\rho = 25$ kN/m^3.

Buildings over Soil Modeled as 3D FEM

In this example, two buildings with different structural systems and different heights were considered. The first building structural system was a bare frame, whereas the second one was a frame with shear-wall shaft, as presented in Fig. 9. We considered a different number of stories for each building (i.e., 4 and 16 stories). The reason behind the selection of 4 and 16 stories was to demonstrate the effect of considering soil–structure interaction (SSI) on the low-

Table 6. Fundamental time periods (s)

Base condition	6-story		12-story	
	Reference (Abdel Raheem et al. 2015)	Proposed approach	Reference (Abdel Raheem et al. 2015)	Proposed approach
Fixed	0.98		1.92	
Stiff soil	1.07	(+5%) 1.03 [–4%]	2.15	(+4%) 2.00 [–7%]
Medium soil	1.12	(+9%) 1.07 [–4%]	2.32	(+18%) 2.26 [–3%]
Soft soil	1.21	(+15%) 1.13 [–6%]	2.60	(+27%) 2.44 [–6%]

Note: Values in parentheses indicate percentage with respect to the fixed-base model; values in brackets indicate percentage with respect to the model (Abdel Raheem et al. 2015).

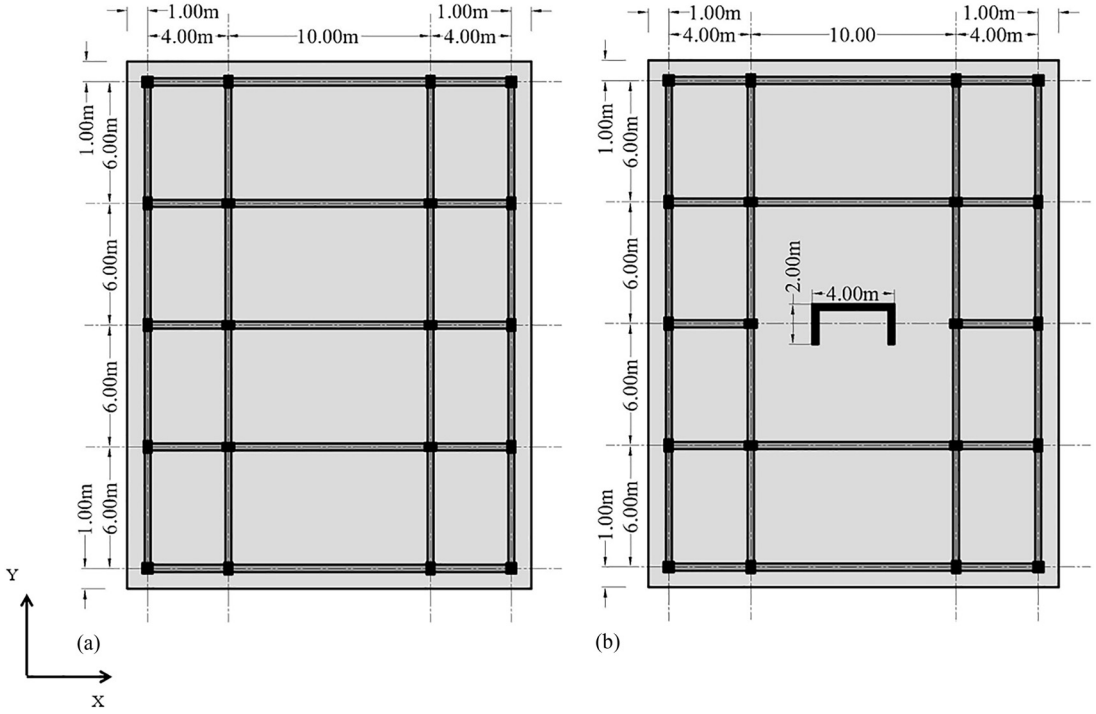

Fig. 11. Structural layout and dimensions: (a) bare frame; and (b) frame with shear wall.

and medium-rise buildings. The results obtained from the proposed approach were compared to the numerical model presented by Jayalekshmi and Chinmayi (2014), in which the building was modeled over soil represented as 3D FEM using the LS-DYNA software. The model properties are given in Tables 1 and 2. The live load was assumed to be 2.75 kN/m, the thickness of the slabs was 0.15 m, and the thickness of the raft was 0.3 m. The results are presented in Table 3.

In this example, we demonstrated that the proposed approach had good agreement with the results of the full 3D approach and can accurately capture the fundamental time period, hence more accurate dynamic behavior can be determined. To the best of our knowledge, we considered the work by Jayalekshmi and Chinmayi (2014) as a reference. The results demonstrated good approximation of the supporting soil compared to the fixed-base model. We argue that the error that was 14% at maximum was due to neglecting the effect of the rotational DOFs in the overall stiffness during the analysis. We showed that when using different kinds of soil, the effect of the rotational stiffness was at a peak when using rock soil but was on the conservative side because the rotational DOF can be considered almost fixed. Although we neglected the effect of the rotational stiffness in the analysis, the proposed approach still gives more accurate results (higher time period compared to the fixed-base model) and hence a more economic design, especially in the case of large-scale buildings.

Building over Soil Modeled as Winkler's Soil Model

The previous example demonstrated a comparison between the results of the analysis using the proposed approach and those of the full 3D approach (direct approach). In this example, the proposed-approach results were compared to those obtained from a building resting over soil idealized as Winkler's springs according to Abdel Raheem et al. (2015).

In this example, the framed building in Fig. 10 is presented. We considered two buildings with a different number of stories (i.e., 6 and 12). The proposed approach results were compared to those of Abdel Raheem et al. (2015) in terms of fundamental time period. The cross-sectional properties and soil modulus of elasticity are given in Tables 4 and 5, respectively. The building was assumed to be subjected to 1.5 kN/m^2 as a flooring load, 10 kN/m as beam and wall loads, and 2.0 kN/m^2 as a live load. The used design acceleration was $0.1a_g$, and the soil class was C, with a damping correction factor of 1.

Table 6 demonstrates the time period results. It can be seen that a good agreement was achieved between the results of the two approaches. Also, the effect of considering the soil and foundation flexibility produced over 20% error compared to the traditional fixed-base model. It has to be noted that despite the good agreement between the results of these approaches, the proposed approach still had superiority in terms of model size and, hence, the computational time and is therefore suitable for large-scale buidlings. Also, the

Table 7. Cross-sectional properties

Element	Dimensions (m)
Slabs	0.2
Beams	0.3 × 0.7
Corner columns	0.5 × 0.5
Other columns	0.4 × 0.7
Raft	1.2

Table 8. Soil properties

Soil type	E (kN/m^2)	ν
Very stiff	200,000	0.25
Stiff	100,000	0.25
Medium	50,000	0.40
Soft	20,000	0.40

Table 9. Fundamental time periods (s)

Structural system	Soil modulus of elasticity [E (kN/m^2)]	Fixed-base model	Conventional iterative approach	Proposed approach	Full 3D finite-element model		
					Meshing size (m)		
					$1 \times 1 \times 2$	$1 \times 1 \times 1$	$0.5 \times 0.5 \times 2$
Frame	20,000	2.64	2.89 (15)	2.94 [2]	3.05	3.04	3.1
	50,000		2.71 (12)	2.80 [2]	2.84	2.83	2.86
	100,000		2.69 (12)	2.74 [2]	2.77	2.77	2.76
	200,000		2.65 (18)	2.69 [2]	2.71	2.7	2.74
Frame with shear wall	20,000	1.13	1.64 (15)	1.72 [2]	1.99	1.95	2.02
	50,000		1.44 (12)	1.47 [2]	1.60	1.62	1.65
	100,000		1.30 (12)	1.38 [2]	1.47	1.42	1.43
	200,000		1.21 (12)	1.33 [2]	1.37	1.36	1.39

Note: Values in parentheses indicate number of iterations required using the conventional substructuring approach; values in brackets indicate number of iterations required using the proposed approach.

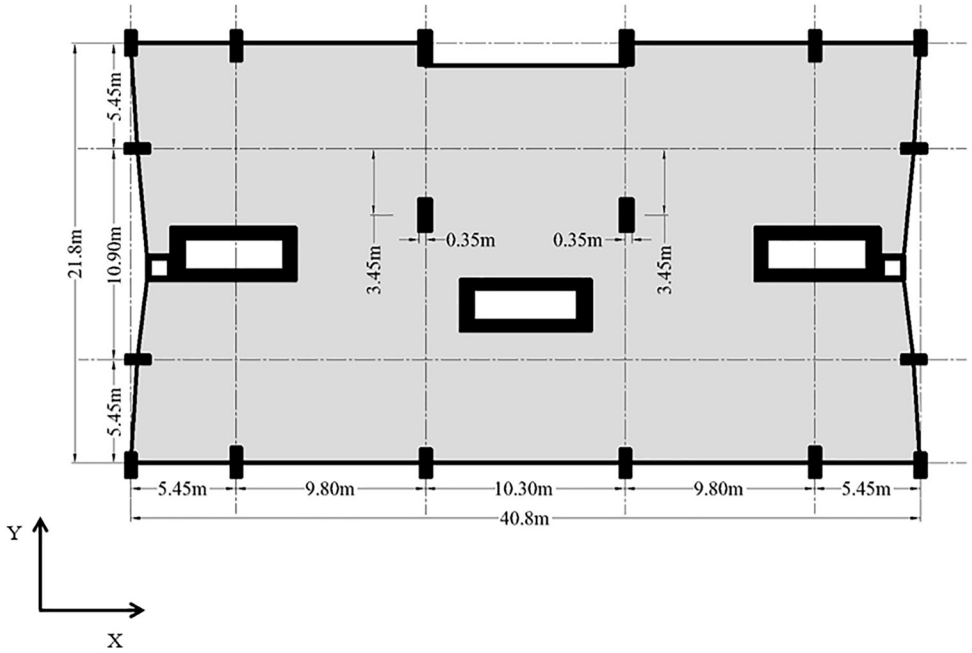

Fig. 12. Structural layout and dimensions of Practical building 1.

approach described by Abdel Raheem et al. (2015) neglected the effect of coupling between the springs, which was not the case in the proposed approach. This will affect the behavior of the raft itself. However, we present only the results in terms of fundamental time period for the sake of clarity and to concentrate on the purpose of this article.

Comparison to Conventional Iterative Method

The previous examples demonstrated the comparison between the results of the analyses using the proposed approach and those of the analyses using approaches described in previously published research. In this example, the proposed-approach results were compared to results obtained using the conventional iterative approach, which is traditionally used in design companies (recall the "Introduction"). This example comprised two different examples with different structural systems. The first was a framed structure, whereas the second was a framed structure with a shear wall, as presented in Fig. 11. The considered building had 10 stories and was assumed to be subjected to 3 kN/m^2 as a flooring load and 10 kN/m^2 as a live load. The section properties and soil modulus of elasticity are presented in Tables 7 and 8, respectively. Also, the full 3D approach (direct approach) using FEM was implemented in this example for the sake of results verification. Three different meshes were used with sizes of $0.5 \times 0.5 \times 2$ m, $1 \times 1 \times 2$ m, and $1 \times 1 \times 1$ m. Table 9 demonstrates the time periods and the required number of iterations.

In this example, we used the full 3D approach (direct approach) as the reference model. We performed convergence study using three different mesh sizes to capture more accurate time periods. We compared the proposed approach with the iterative substructuring approach widely used in design companies (recall the "Introduction"). In this example, we demonstrated that the proposed approach converged faster than the iterative substructuring approach mentioned in the literature (2 iterations versus 12 iterations as the best case). In addition, the iterative substructuring approach showed poor accuracy in terms of time periods (it was almost similar to the fixed-base model) with respect to the full 3D model. Also, the problem to be solved was much larger than the

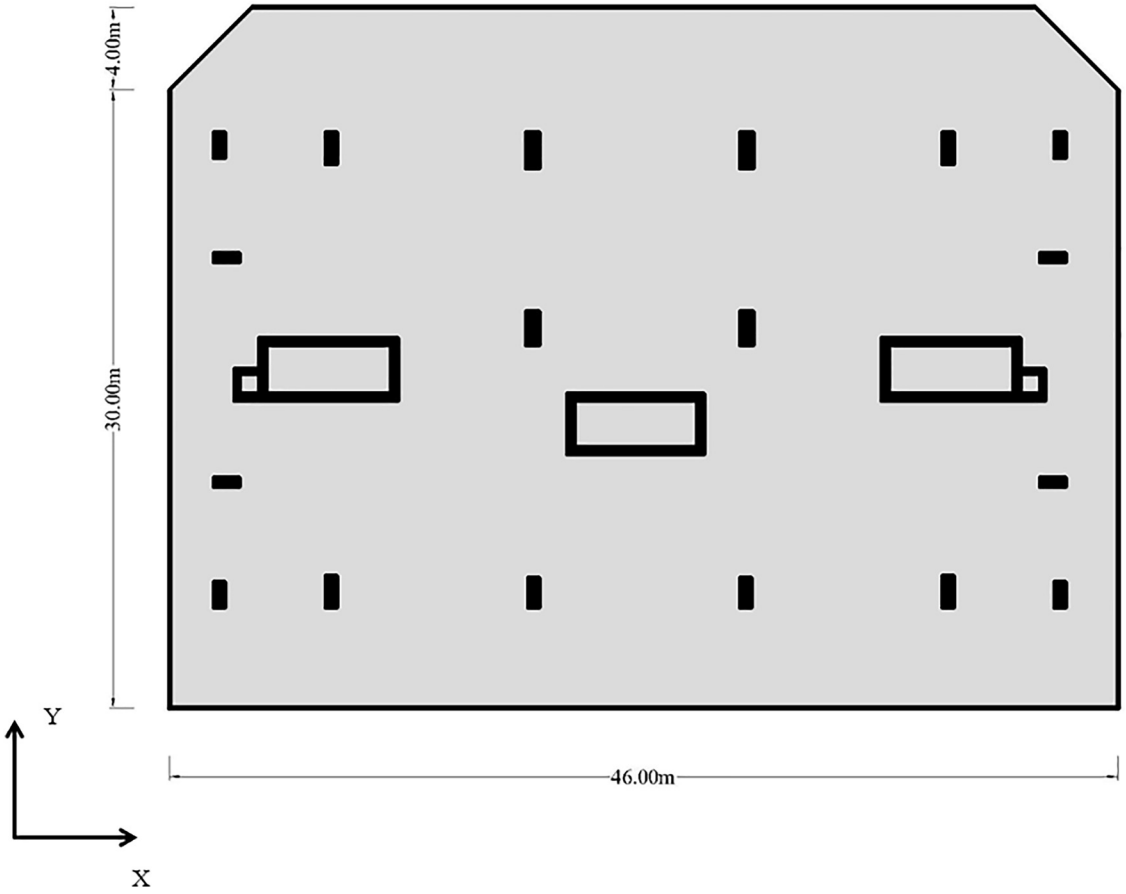

Fig. 13. Foundation layout of Practical Building 1.

Table 10. Properties of Practical Building 1

Property	Value
Number of stories	20
Total height (m)	60
Floor height (m)	3
Wall thickness (m)	0.3
Slab thickness (m)	0.2
Raft thickness (m)	2
Soil of modulus elasticity (t/m^2)	5,000
Type of seismic analysis	Response spectrum
Seismic code	Eurocode 8
Response reduction factor	1
Dead load (t/m^2)	0.2
Live load (t/m^2)	0.3
Design ground acceleration	0.1
Subsoil class	C
Damping correction factor	1

Table 11. Fundamental time periods (s)

Direction	Fixed base	Proposed approach	Conventional iterative technique
X-direction	1.62	2.79 [+72%]	1.83 [+13%]
Y-direction	2.33	3.09 [+33%]	2.48 [+6%]

Note: Values in brackets indicate reduction/increase in time period with respect to the fixed-base model.

Table 12. Nonscaled base-shear demand (tons)

Load case	Corresponding direction	Fixed base	Proposed approach	Conventional iterative technique
Load in *X*-direction	*X*-direction	230.16	167.4 [–73%]	224.02 [–3%]
Load in *Y*-direction	*Y*-direction	137.54	98.31 [–29%]	111.18 [–19%]

Note: Values in brackets indicate reduction/increase in base shear with respect to the fixed-base model.

same problem when using the proposed approach specifically for a large-scale building on a raft foundation. This means that the proposed approach is scalable (i.e., the number of iterations is independent of the size of the problem and the mesh size of the raft foundation, as we demonstrate in the following two examples).

Practical Building 1

The previous examples presented, to some extent, theoretical comparisons and verifications of the analysis using the proposed approach. The purpose of these two examples (this one and the next) is to demonstrate the use of the proposed approach in practical structural engineering and its scalability and to demonstrate how much decrease in the design base shear could be achieved.

Fig. 14. Structural layout and dimensions of Practical Building 2.

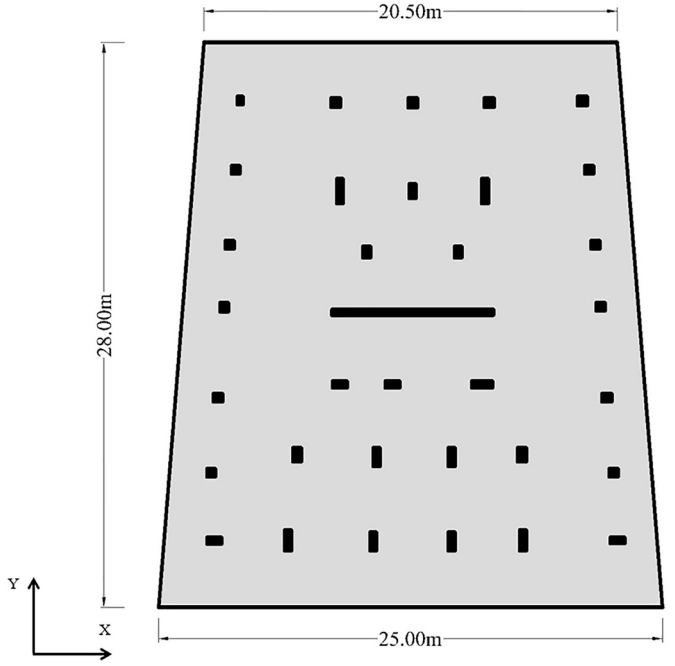

Fig. 15. Foundation layout of Practical Building 2.

In this example, the time period and the corresponding base shear for an actual practical building consisting of 20 stories was demonstrated. Three approaches were considered in the comparison: the fixed-base model, the proposed approach, and the conventional iterative approach. The building plan and the building's foundation are presented in Figs. 12 and 13, respectively. The properties used in this example are given in Table 10.

Tables 11 and 12 demonstrate the results in terms of time periods and base shear, respectively. It can be seen from the results that the time period considering the soil and foundation flexibility was increased. This led to a substantial decrease in the base shear (over 70% in some cases). This could be useful for the purpose of value engineering. Also, the convergence in this example was achieved after two iterations, which illustrates the scalability of the proposed approach.

Practical Building 2

In this example, an actual practical building consisting of 20 stories was analyzed using the fixed-base model, the proposed approach, and the conventional iterative approach. Similar to the previous example, the comparison was carried out to obtain the time period and the corresponding base shear. The building's plan and foundation are demonstrated in Figs. 14 and 15, respectively. The properties used in this example are given in Table 13.

Tables 14 and 15 demonstrate the results in terms of time periods and base shear, respectively. Again, it can be seen from the results that the time period considering the soil and foundation flexibility was increased. This led to a substantial decrease in the base shear (over 43% in some cases). Also, the convergence in this example was achieved after two iterations, which illustrates the scalability of the proposed approach.

Table 13. Properties of Practical Building 2

Property	Value
Number of stories	20
Total height (m)	60
Floor height (m)	3
Wall thickness (m)	0.25
Slab thickness (m)	0.25
Raft thickness (m)	2
Soil of modulus elasticity (t/m^2)	10,000
Type of seismic analysis	Response spectrum
Seismic code	Eurocode 8
Response reduction factor	1
Dead load (t/m^2)	0.2
Live load (t/m^2)	0.3
Design ground acceleration	0.1
Subsoil class	C
Damping correction factor	1

Table 14. Fundamental time periods (s)

Direction	Fixed base	Proposed approach	Conventional iterative technique
X-direction	1.99	2.79 [+40%]	2.33 [+17%]
Y-direction	2.71	3.21 [+18%]	2.88 [+17%]

Note: Values in brackets indicate reduction/increase in time period with respect to the fixed-base model.

Table 15. Nonscaled base-shear demand (tons)

Load case	Corresponding direction	Fixed base	Proposed approach	Conventional iterative technique
Load in *X*-direction	*X*-direction	265.32	150.29 [–43%]	219.82 [–17%]
Load in *Y*-direction	*Y*-direction	149.38	127.45 [–15%]	148.10 [–0.1%]

Note: Values in brackets indicate reduction/increase in base-shear with respect to for the fixed-base model.

Implementability in Practice

The generality of the proposed method was discussed in the previous sections, and as mentioned in the "Limitations and Remarks" section, it is guaranteed that whenever two software programs (one for the analysis of the superstructure and the other for analysis of the raft foundation on EHS) are available, the implementation is straightforward and needs no special work other than the work designers do in their daily routines. To be specific, the way practitioners may use this method is first to solve the superstructure as demonstrated in Step 0 in the "Proposed Procedure for Evaluating Time Periods of Tall Buildings" section using any of the available building analysis software, and then using some method to extract the reactions and invert them to the foundation–soil problem. After that, the foundation–soil problem can be solved using any available software for that purpose, as demonstrated in Step 1 in the section on the proposed procedure. These two steps should be repeated in a recursive manner till the convergence is achieved. This convergence can be decided based on the designer's experiences and preferences. However, the only available software that can do this automatically with minimum effort is available from Elmeliegy and Rashed (2017).

Concluding Remarks and Recommendation for Further Work

In this paper, we proposed a new preconditioned iterative domain decomposition technique based on substructuring, named PSSI, for buildings over raft foundations. The new preconditioned iterative substructure approach is based on placing the separation cut at the column–raft interface instead of the raft–soil interface in the conventional iterative approach. Using this technique, we were able to limit the interface problem size to the number of vertical supporting elements (columns and shear walls), hence reducing the number of variables needed to iterate them. Consequently, the number of iterations required to converge to two iterations only was reduced in most cases. The proposed-approach results were compared to those obtained from different models and techniques, including the fixed-base model, Winkler's model, the conventional iterative approach, and the full 3D FEM approach. The proposed-approach results demonstrated—over the conventional iterative approach—a good agreement with those of the full 3D FEM approach, with an approximate average error within 10%. It can be seen that, considering a different number of stories and different structural systems, the proposed approach requires only two iterations, whereas the conventional iterative one requires at least 10 iterations to obtain stable results.

It can be seen from the results in the last two examples that there was an increase in time period that reached, in some cases, 70%, which in turn decreased the base shear by approximately 70%. This could be useful for the purpose of value engineering. Not only did the practical examples show that the proposed approach herein can be used in practice by modelers and structural engineers, they also provided evidence of the scalability of that approach (i.e., the number of iterations was independent of the size of the problem), which makes the proposed approach better than the conventional iterative approach.

It should be noted that, for buildings with more complexity (for example, frames with setbacks or walls with bracing), the convergence may not be achieved in exactly two iterations. However, based on the manner of substructuring, a minimal number of DOFs is always taken into consideration. In addition, because the vertical DOFs can capture the effect of the foundation–soil flexibility effectively, as discussed in the "Limitations and Remarks" section and shown in the examples, the authors claim that this method should converge faster than the existing practical methods in the literature.

The superiority of the proposed approach can be summarized as follows:

1. The interface problem size is much smaller than that resulting from the conventional iterative approach, hence less computational time and less storage space are required.
2. Due to the substantial decrease in the problem size (the stiffness matrix of the interface problem becomes smaller), the number of iterations required for convergence is substantially decreased.
3. Providing that we support the proposed approach with a simple GUI, this approach can be easily used by engineers in practice.
4. Although we used ETABS and PLPAK in this work to introduce and validate this approach, the approach can be applied easily to any other software that has similar capabilities without losing generality.

It should be noted that, although we did not include the damping and nonlinear soil–structure interaction in the developed technique, such extensions are subjects of ongoing research.

Finally, although this study introduced the analysis of buildings over raft foundations, the extension to a piled raft is trivial and needs no special implementation once one has software to solve the

piled-raft foundation without losing generality. In other words, the proposed method is an iterative static-condensation method; therefore, whatever happens in the structure or in the foundation soil, the proposed method works. However, one may expect a slight change in the convergence rate compared to the other methods in the literature.

Acknowledgments

The first author thanks Dr. Taha H. A. Naga for the intriguing discussions and Anas Abourawash for help in the design of the GUI. Also, the authors thank ACE Consulting Engineers–Moharram Bakhoum for providing the licenses for CSI ETABS. Finally, the authors thank the anonymous reviewers for their valuable comments that made this work written in this form.

References

Abdel Raheem, S. E., M. M. Ahmed, and T. M. A. Alazrak. 2015. "Evaluation of soil–foundation–structure interaction effects on seismic response demands of multi-story MRF buildings on raft foundations." *Int. J. Adv. Struct. Eng.* 7 (1): 11–30. https://doi.org/10.1007/s40091-014-0078-x.

BE4E. 2017. "Iterative soil-structure interaction tool." Accessed April 5, 2016. http://www.be4e.com/new/Iterative.html.

Bhattacharya, K., S. C. Dutta, and S. Dasgupta. 2004. "Effect of soil-flexibility on dynamic behaviour of building frames on raft foundation." *J. Sound Vib.* 274 (1–2): 111–135. https://doi.org/10.1016/S0022-460X(03)00652-7.

Bowles, J. E. 1986. *Foundation analysis and design.* 3rd ed. New York: McGraw-Hill.

Colasanti, R. J., and J. S. Horvath. 2010. "Practical subgrade model for improved soil-structure interaction analysis: Software implementation." *Pract. Period. Struct. Des. Constr.* 15 (4): 278–286. https://doi.org/10.1061/(ASCE)SC.1943-5576.0000060.

Computers and Structures Inc. 2011. *Extended three dimensional analysis of building systems (ETABS).* Computer software package, version 9.7.4. Berkeley, CA: Computers and Structures Inc.

Dang, D. N., B. J. Seong, and S. K. Dong. 2013. "Design method of piled-raft foundations under vertical load considering interaction effects." *Comput. Geotech.* 47: 16–27.

Elmeliegy, A. M., and Y. F. Rashed. 2017. *A developed FEM-BEM practical technique to consider SSI in the lateral analysis for multistory buildings: Software implementation.* Giza, Egypt: Cairo Univ.

Gazetas, G. 1991. "Formulas and charts for impedances of surface and embedded foundations." *J. Geotech. Eng.* 117 (9): 1363–1381. https://doi.org/10.1061/(ASCE)0733-9410(1991)117:9(1363).

Gazetas, G., and G. Mylonakis. 1998. "Seismic soil-structure interaction: New evidence and emerging issues." In *Proc., Geotechnical Earthquake Engineering and Soil Dynamics III*. Reston, VA: ASCE.

Hemsley, J. 1987. "Elastic solutions for axisymmetrically loaded circular raft with free or clamped edges founded on Winkler springs or a half-space." *Proc. Inst. Civ. Eng.* 83 (1): 61–90. https://doi.org/10.1680/iicep.1987.342.

Horvath, J. S. 1983. "New subgrade model applied to mat foundations." *J. Geotech. Eng.* 109 (12): 1567–1587. https://doi.org/10.1061/(ASCE)0733-9410(1983)109:12(1567).

Huang, S., O. Ozcelik, and Q. Gu. 2015. "A practical and efficient coupling method for large scale soil–structure interaction problems." *Soil Dyn. Earthquake Eng.* 76: 44–57. https://doi.org/10.1016/j.soildyn.2014.12.014.

Jahromi, H. Z., B. A. Izzuddin, and L. Zdravkovic. 2009. "A domain decomposition approach for coupled modelling of nonlinear soil–structure interaction." *Comput. Methods Appl. Mech. Eng.* 198 (33–36): 2738–2749. https://doi.org/10.1016/j.cma.2009.03.018.

Jayalekshmi, B. R., and H. K. Chinmayi. 2014. "Effect of soil flexibility on seismic force evaluation of RC framed buildings with shear wall: A comparative study of IS 1893 and EUROCODE8." *J. Struct.* 2014: 493745. https://doi.org/10.1155/2014/493745.

Jayalekshmi, B. R., and H. K. Chinmayi. 2016. "Effect of soil stiffness on seismic response of reinforced concrete buildings with shear walls." *Innovative Infrastruct. Solutions* 1: 2. https://doi.org/10.1007/s41062-016-0004-0.

Kalkan, E., and A. K. Chopra. 2010. *Practical guidelines to select and scale earthquake records for nonlinear response history analysis of structures*, 124. USGS Open-File Rep. 2010-1068. Reston, VA: USGS.

Kerr, A. D. 1964. "Elastic and viscoelastic foundation models." *J. Appl. Mech.* 31 (3): 491–498. https://doi.org/10.1115/1.3629667.

Kocak, S., and Y. Mengi. 2000. "A simple soil–structure interaction model." *Appl. Math. Modell.* 24 (8–9): 607–635. https://doi.org/10.1016/S0307-904X(00)00006-8.

Mengke, L., X. Lu, X. Lu, and L. Ye. 2014. "Influence of soil–structure interaction on seismic collapse resistance of super-tall buildings." *J. Rock Mech. Geotech. Eng.* 6 (5): 477–485. https://doi.org/10.1016/j.jrmge.2014.04.006.

Mylonakis, G., and G. Gazetas. 2000. "Seismic soil-structure interaction: Beneficial or detrimental?" *J. Earthquake Eng.* 4 (3): 277–301. https://doi.org/10.1080/13632460009350372.

Mylonakis, G., S. Nikolaou, and G. Gazetas. 2006. "Footings under seismic loading: Analysis and design issues with emphasis on bridge foundations." *Soil Dyn. Earthquake Eng.* 26 (9): 824–853. https://doi.org/10.1016/j.soildyn.2005.12.005.

Pandey, A. K., G. Kumar, and S. P. Sharma. 1994. "An iterative approach for the soil-structure interaction in tall buildings." *Eng. Fract. Mech.* 47 (2): 169–176. https://doi.org/10.1016/0013-7944(94)90218-6.

Rashed, Y. F. 2005. "A boundary/domain element method for analysis of building raft foundations." *Eng. Anal. Boundary Elem.* 29 (9): 859–877. https://doi.org/10.1016/j.enganabound.2005.04.007.

Reissner, E. 1947. "On bending of elastic plates." *Q. Appl. Math.* 5 (1): 55–68. https://doi.org/10.1090/qam/20440.

Shaaban, A. M., and Y. F. Rashed. 2013. "A coupled BEM-stiffness matrix approach for analysis of shear deformable plates on elastic half space." *Eng. Anal. Boundary Elem.* 37 (4): 699–707. https://doi.org/10.1016/j.enganabound.2012.12.005.

Vander Weeën, F. 1982. "Application of the boundary integral equation method to Reissner's plate model." *Int. J. Numer. Methods Eng.* 18 (1): 1–10. https://doi.org/10.1002/nme.1620180102.

Viladkar, M. N., Karisiddappa, P. Bhargava, and P. N. Godbole. 2006. "Static soil–structure interaction response of hyperbolic cooling towers to symmetrical wind loads." *Eng. Struct.* 28: 1236–1251. https://doi.org/10.1016/j.engstruct.2005.11.010.

Wang, C. M., Y. K. Chow, and Y. C. How. 2001. "Analysis of rectangular thick rafts on an elastic half space." *Comput. Geotech.* 28 (3): 161–184. https://doi.org/10.1016/S0266-352X(00)00030-6.

Winkler, E. 1867. *Die lehr von elastizität und festigkeit.* Prague, Austria-Hungary: Dominicius.